Very low thermally induced tip expansion by vacuum ultraviolet irradiation in a scanning tunneling microscope junction

D. Riedel,* C. Delacour, A. J. Mayne, and G. Dujardin
Laboratoire de Photophysique Moléculaire, CNRS-UPR 3361, Bâtiment. 210, Université Paris Sud, 91405 Orsay, France
(Received 16 June 2009; revised manuscript received 26 August 2009; published 28 October 2009)

The thermal and photoelectronic processes induced when a vacuum ultraviolet (VUV) laser irradiates the junction of a scanning tunneling microscope (STM) are studied. This is performed by synchronizing the VUV laser shots with the STM scan signal. Compared to other wavelengths, the photoinduced thermal STM-tip expansion is not observed when the VUV radiation is freed from spurious emissions. Furthermore, we demonstrate that the purified VUV photoinduced transient signal detected in the tunnel current is entirely due to photoelectronic emission and not combined with thermionic processes. The ensuing photoelectron emission is shown to be independent of the tip-surface distance while varying linearly with the pure VUV laser intensity. These results illustrate a strong decoupling between phonons and photoelectrons which allows a very weak STM-tip expansion.

DOI: 10.1103/PhysRevB.80.155451 PACS number(s): 41.20.Jb, 72.40.+w, 82.37.Gk

I. INTRODUCTION

The laser irradiation of a scanning tunneling microscope (STM) junction has often been investigated in various configurations with a common motivation of combining high spatial resolution of the STM with the spectral or temporal resolution of the laser.[1–7] In many of these experiments, in which generally visible or infrared wavelengths are used, it is frequently considered that the various photoinduced effects such as electron-phonon coupling,[8,9] photovoltage,[10] thermovoltage,[11] photoelectron emission,[12] hot electron formation,[13] and tunnel current rectification[14] are decoupled. Thus, in many experiments, the optical-field confinement and enhancement that may be created underneath the STM-tip apex[15,16] is regularly considered as an independent optical process separated from the other photoinduced effects.[6,15,17–19] In particular, photoinduced thermal expansion of the STM-tip, usually caused by electron-phonon coupling, is one of the most important and correlated effects commonly encountered in such laser-STM experiments, even for an ultrashort laser pulse irradiation.[8] To have a better control over these correlated properties, new investigation route can be proposed when exploring the use of other irradiation wavelengths.[20,21]

In this work, we report an original method of laser-STM combination that allows measuring the photoinduced STM-tip expansion when associated with photoelectronic emission. This is performed by exposing the junction of a room-temperature STM to a pulsed vacuum ultraviolet (VUV) laser. To decouple the observation time scale between thermal and electronic effects, we trigger the laser shots via the lateral STM-tip scanning signal acquired during STM topography. In addition, the spectral separation of the optical signal between the pure VUV emission and spurious visible and infrared (IR) wavelengths shows that visible and IR wavelengths provoke a strong STM-tip expansion while pure VUV radiation produces merely photoelectron emission. The ensuing pure VUV photoinduced electronic signal is shown to be independent of the tip-surface distance whereas it varies linearly with the laser intensity. Furthermore, the simulation of the transient response of our measurement chain demonstrates that this photoelectron emission is not combined with thermionic processes. These results are robust indications that the VUV induced photoelectrons are strongly decoupled from thermal effects and mainly produced from the irradiated side of the STM-tip surface, far from the tip-apex region. The ensuing nonobservable STM-tip expansion that occurs when the pure VUV beam irradiates the STM junction may indicate a specific low electron-phonon coupling at the tungsten STM-tip surface since the energy densities used for both types of the wavelengths used are identical. It is suggested that the observed surface photoelectron emission, which is a one-photon process in our experimental conditions, might be related to this low electron-phonon energy transfer.

II. EXPERIMENTS

Experiments are performed with an ultrahigh vacuum room-temperature STM (OMICRON) described previously.[22,23] An F_2 excimer laser beam ($\lambda=157$ nm, 7.9 eV, Excistar M100, and pulse duration of ~ 10 ns) propagates toward the STM through vacuum and irradiates the STM junction composed of a tungsten tip and a Si(100)-(2 $\times 1$):H surface (n type, As doped, and 4–6 mΩ cm).[22,24] An F_2 excimer laser beam and three aluminum mirrors providing a p polarization are combined with a CaF_2 lens ($f=750$ mm) to focus the pure VUV beam ($d\sim 1$ mm) on the STM junction with an electric field oriented along the STM-tip axis direction [Fig. 1(a)]. For mechanical reasons, the incident angle of the laser beam is $\sim 62°$ relative to the normal of the silicon surface. In addition to the experimental setup described in Ref. 22, one aluminum mirror can be replaced with an MgF_2 Pellin-Brocca (PB) prism allowing the visible and IR emissions generated by the excimer laser cavity to be separated. Although the initial VUV energy per pulse is much higher than the spurious IR and visible radiations, the VUV is strongly attenuated during its propagation via optical components. In these conditions, the measured optical energy density (fluence per laser pulse) of the

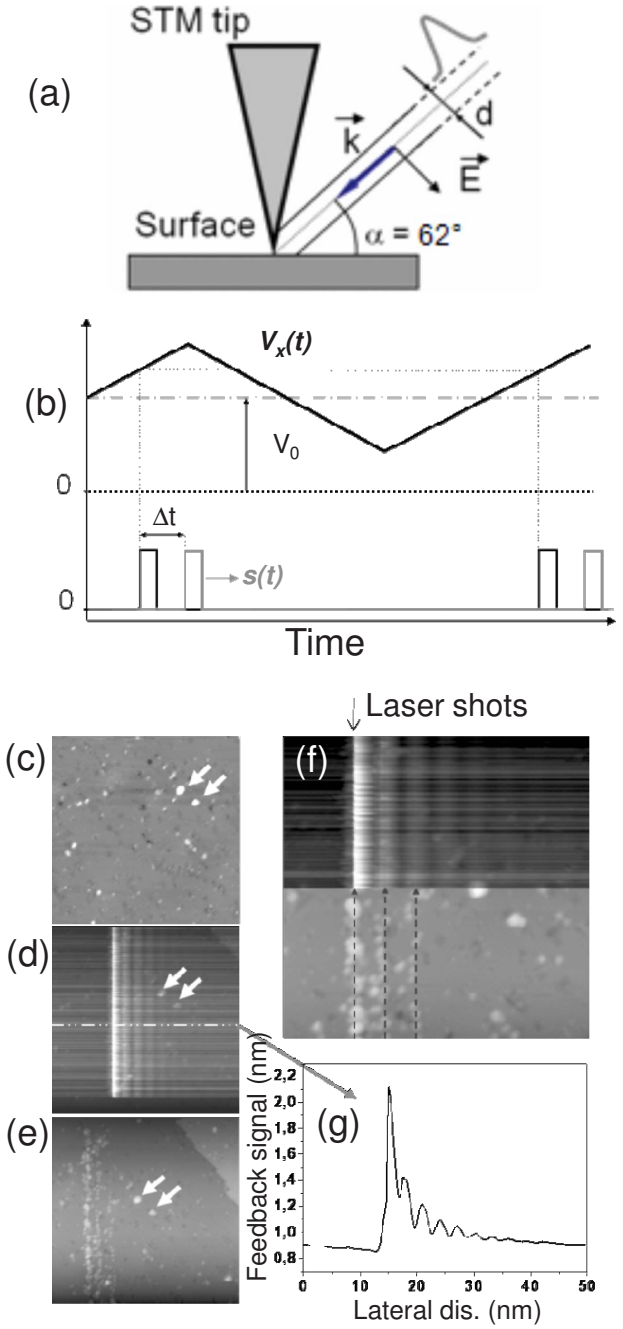

FIG. 1. (Color online) (a) Schematic view of the scanning tunneling microscope irradiation conditions showing the collimated VUV beam waist of diameter $d \sim 1$ mm irradiating the STM junction with a an incident angle of 62° and a polarization orientated along the STM-tip axis. (b) Chronograph of the horizontal STM scanning signal $V_x(t)$ and the corresponding fabricated triggering signal $s(t)$. (c)–(e) are 50×50 nm^2 STM topographies ($V_s = -1.5$ V, $I = 200$ pA) of the Si(100):H surface before irradiation, during the laser irradiation and after irradiation, respectively (the arrows indicate landmark positions). (f) 30×30 nm^2 STM topography comprising the upper part of (d) and the lower part of (e), respectively. (g) Averaged profile derived from the dashed lines [see (d)] as a function of the lateral distance. Note that the feedback signal, originally measured in volts, is converted in nm after a precise calibration of the STM-tip z-piezo actuator on a Si(100):H surface step edge.

pure VUV radiation applied to the STM junction (~ 10 mJ/cm^2) is identical to the measured fluence which takes into account, after separation with the PB prism, the visible and IR radiations. For accurate optical adjustment, the PB prism and the last mirror mount are motorized with precise piezoelectric actuators. This setup allows adjusting, horizontally and vertically, the position of the pure VUV beam waist, as well as the IR and visible wavelengths, to assure a perfect match of the two optical spots on the STM junction. The positioning of the pure VUV beam is performed by precisely placing, via a telescope, a photoinduced fluorescence spot on a quartz sample surface fixed parallel to the silicon sample and thus aligned with the STM junction. IR and visible radiations are adjusted in the same way when a red spot is directly observed on the silicon sample and centered on the STM-tip-sample junction, similarly to what is done in Ref. 25. Note that these adjustments are eased by the larger beam waist of the pure VUV ($d \sim 1$ mm) and the IR and visible wavelengths ($d \sim 5$ mm) compared to the STM-tip diameter ($d \sim 0.1$ mm). Various measurements have been performed with slight misalignments of these optical spot positions without any noticeable differences. Several tungsten tips have been used for these experiments. Each of them has been carefully cleaned by electron bombardment to remove the tungsten oxide layer at the apex and on the side of the STM tips. None of the tested STM tips, which might have slightly different shapes, have induced changes in the observed results.

III. RESULTS AND DISCUSSION

To study the photoinduced thermal effects on the STM junction, we first synchronized the full excimer laser radiation shots (VUV, visible, and IR emissions) with the lateral motion of the STM tip, so that a single laser pulse can be triggered at any position with a single scanned line. This is achieved by using the lateral scanning saw tooth signal $V_x(t)$ produced by the STM controller to generate electronically a single rectangular voltage pulse $s(t)$ with a chosen delay Δt [Fig. 1(b)]. When $s(t)$ is used to trigger the laser, we can allocate a series of single laser shots to a line perpendicular to the STM scan direction as shown in Fig. 1(d). The selected delay Δt allows the laser line shots to be placed at any position in the STM topography. To measure the laser-induced tip-surface distance perturbation, we first acquired an STM topography of the hydrogenated Si(100)-(2×1):H surface without laser shots [Fig. 1(c)]. Then the VUV laser is triggered during a second scan of the same area [Fig. 1(d)]. In this figure, the initial bright line corresponds to the laser impact on the STM junction, while additional damped oscillations parallel to the line of laser shots are observed (the STM scans from left to right).

Since the STM topographies are performed in constant current mode, the observed damped oscillations correspond to tip height variations occurring a long time after the laser pulse strike the STM junction. Thus, following the laser perturbation, a bright feature implies a strong reaction of the STM feedback loop signal to correct the tip-surface distance. After the irradiation of the STM junction, the STM topogra-

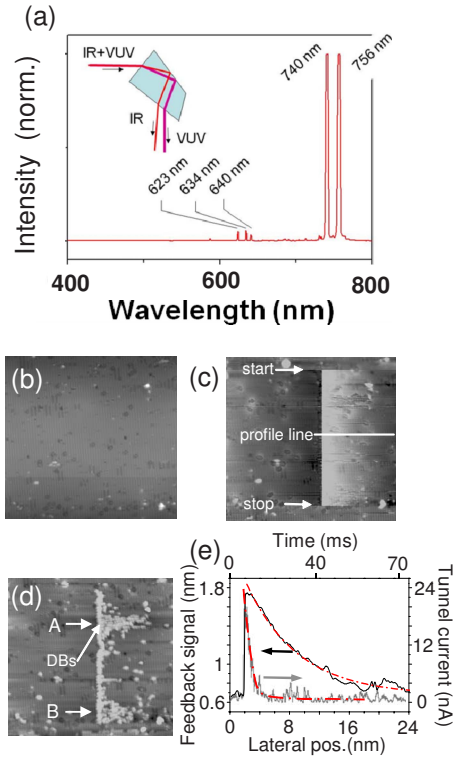

FIG. 2. (Color online) (a) Visible-IR spectrum of the spurious excimer cavity emission before separation by a Pellin-Broca prism (see the inset). (b)–(d) 50×50 nm^2 STM topographies (V_s= −1.5 V, I=200 pA) of the Si(100):H surface before, during, and after the STM junction irradiation with the IR and visible light radiations, respectively. During (c), the surface voltage has been changed shortly (a few line scans) from −1.5 to −3.5 V (and reverse) resulting in the observable hydrogen desorption variation as indicated by arrows A and B in (d). (e) Recorded feedback signal following the laser shots, taken from the profile of (c) and the corresponding tunnel current during a corresponding line scan. Note that the red curves in (e) correspond to numerical fits of the feedback and current signals with a single exponential decay function.

phy of the same area shows irregular hydrogen desorption lines having the same direction as the STM-tip height damped oscillations [Fig. 1(e)]. By superimposing precisely the STM topographies comprising the top part of Fig. 1(d) and the lower part of Fig. 1(e) we can see in Fig. 1(f) that the position of the dehydrogenated lines match the maxima of the feedback signal. Indeed, the feedback signal reaches maximum, when the tip-surface distance is minimum, i.e., when the tunnel current is high. To check that the observed white lines correspond to dehydrogenated silicon dimers (i.e., dangling bonds of the silicon surface), hydrogen hopping is provoked by imaging at a surface voltage $V_s>-2.5$ V (not shown).[23]

To further discriminate between photoinduced heating process and photoinduced electronic emission, we optically purified the laser beam by separating the pure VUV wavelength from other light emissions present in the laser cavity formed during the excimer gas discharge [see the inset of Fig. 2(a)]. Indeed, as shown in Fig. 2(a), the spectrum of the VUV laser beam presents a number of visible and IR emissions in the range of 400–800 nm, which are mainly due to radiation from excited fluorine atoms F*. Thus, the precise rotation of the MgF_2 PB prism allows lighting the STM junction with either the pure VUV beam or the IR and visible lights.

When the non-VUV radiation hits the STM junction, similarly to what is done in Fig. 1(d), the corresponding feedback signal can be recorded through the series of STM topographies shown in Figs. 2(b)–2(d). After irradiation, the STM topography of Fig. 2(d) shows a clear dehydrogenation line while the recorded profile of the feedback signal [Fig. 2(c)] shows an exponential decaying behavior [Fig. 2(e)]. The STM-tip scanning speed (150 ms/line) allows us to ascribe an exponential decay constant of ~36 ms to the feedback signal while the transient current trace can be similarly fitted with an exponential decay constant of ~4.8 ms. Note that the dehydrogenation process can occur a long time after the laser pulse [see positions A and B in Fig. 2(d)] when the surface voltage is changed from −1.5 to −3.5 V during the scan.

However, when the purified VUV laser beam is directed onto the STM junction, we record a rapid transient signal in the tunnel current and the corresponding feedback response. As observed in Fig. 3(a), the time scale of these signals is much shorter than the one observed in Fig. 2(e). Indeed, the corresponding feedback response shows a delay time of ~1340 μs while the tunnel current peak depicts a duration of ~392 μs (full width at half maximum), which is ten times smaller than the exponential decay constant observed in the current trace of Fig. 2(e). Note that the photoelectron signal can be observed, with the same intensity, whether the STM tip is in tunnel mode or not. The related feedback response can also be observed during the STM topography when the laser is triggered along a line similar to that shown in Figs. 1(d) and 2(c). Yet, neither hydrogen desorption nor damped oscillations are observed in the STM topography following pure VUV irradiation [Fig. 3(b)] while the same optical fluence is applied into the STM junction in both cases, and even for surface voltage of V_s=−2.5 V [see Fig. 2(d) for comparisons]. This result suggests that the photoirradiation of the STM junction induces STM-tip expansion only when visible or IR wavelengths are used while no expansion seems to occur when pure VUV is employed. Thus, the hydrogen desorption observed in Figs. 1(e) and 2(d) is believed to be induced by the sudden STM-tip expansion following the IR and visible irradiations of the STM junction. Indeed, the subsequent shorter tip-surface distance increases locally the tunnel current while the surface voltage (V_s=−1.5 V) remains unchanged [Figs. 1(d) and 2(e)]. However, such a low surface voltage is usually inadequate to induce hydrogen desorption.[26,27] In the present case, the hydrogen desorption efficiency can be significantly increased if the tunnel electron flux rapidly reaches several nA's [Fig. 2(e)]. This process is further confirmed by the higher desorption efficiency for absolute higher surface voltage as observed in Fig. 2(d).

The feedback oscillations observed in the STM topographies of Figs. 1(d) and 1(f) suggest that the feedback loop is acting—in a transient way—on the STM-tip vertical displacement, a long time after the laser irradiation, to recover its initial position. Note that the feedback loop parameters

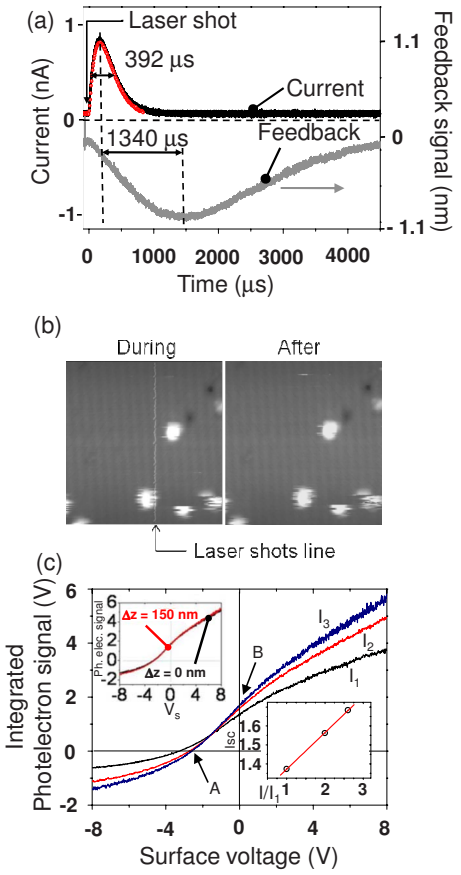

FIG. 3. (Color online) (a) Transient variation in the STM current signal and the corresponding feedback response (V_s=0) as functions of time following a pure VUV laser pulse. The red curve is the response of the current measurement chain when excited by a 10 ns voltage pulse (100 mV). (b) 12×12 nm^2 STM topographies on Si(100):H surface, during (left) and after (right) pure VUV laser shots synchronized on a line (V_s=−2.5 V, I=200 pA). (c) Variation of the integrated photoelectrons signal [black curve of (a)] as a function of the STM junction surface voltage for two different tip-surface distances (upper left inset) and for three different VUV laser intensities I_1, I_2=2I_1, and I_3=2.6I_1 (lower right inset). A and B arrows indicate the equivalent open circuit voltage and the short-circuit current, respectively.

are kept constant during these experiments. Thus, the absence of observable oscillations in the STM topography in Figs. 2(c) and 3(b) indicates that a specific damping process occurs when both irradiations hit the STM junction. It appears that, in this latter case, the rapid photoinduced VUV transient current response is perturbing the feedback loop correction of the long time scale photoinduced thermal expansion. A precise study of these dynamical feedback processes is planned for a future paper.

The time scale of the transient tunnel current signal shown in Fig. 3(a) is, however, much longer than expected for a photoelectronic emission induced during a laser pulse duration of ~10 ns. This might originate from a VUV photoelectron emission combined with a delayed photoinduced thermionic process. This time broadening can also simply be due to the limited bandwidth of the preamplifier (cutoff frequency f_c~50 kHz) and the low-pass filter (f_c~1.3 kHz) that are used to measure this signal, if only pure photoelectron emission occurs. To discriminate between these two processes, we simulated the transient response of our measurement chain (preamplifier and low-pass filter) by applying a 10 ns voltage pulse (100 mV) in series with a 0.5 GΩ resistor at the entrance of the preamplifier. The resulting output signal is very similar to the observed transient current response measured when the STM junction is irradiated by the pure VUV wavelength [red curve in Fig. 3(a)]. This indicates that this photoinduced transient current signal is mainly due to a pure photoelectron emission rather than a rapid heating and a quick thermal relaxation of the STM-tip expansion as proposed in Ref. 12. It thus rules out the possibility of thermionic emission.[28] In these conditions, the delayed feedback signal observed in Fig. 3(a) is a direct signature of the STM feedback loop corrector in response to the transient photocurrent peak rather than a response to a STM-tip expansion.

To investigate the properties of this photoelectron signal, we plot the variation of the integrated transient VUV photoinduced tunnel current trace [black curve in Fig. 3(a)] as a function of the surface voltage V_s for two variable parameters: the tip-surface distance and the laser intensity [Fig. 3(c)]. This is performed by a box car integrator (Princeton Applied Research, M360), with an integration window of 1 V and a duration of 1 ms. The ensuing integrated photoelectron signal slowly varies with the surface voltage while it is shown to be independent with the tip-surface distance [see the left inset of Fig. 3(c)]. Other shorter tip-surface distances (i.e., in tunnel regime) show similar curves but are not plotted for clarity. Therefore, photoemission from the apex of the STM tip resulting from a possible confined optical field is assumed to be negligible, compared to the strong emission that occurs from the illuminated side of the STM tip.[29]

When the laser intensity varies from I_1 to I_2=2I_1 or I_3 =2.6I_1 the integrated photocurrent signal shows a characteristic behavior, which is very similar to a photodiode junction I-V curves for various illumination intensities.[30] The equivalent open circuit voltage V_{oc} (photocurrent equals zero) is indicated by the A arrow in Fig. 3(c). In our specific case, these values give insight on the measured photoelectron kinetic energy: from the work function of the clean tungsten tip (~4.55 eV) and the energy of the VUV photons (~7.9 eV), the deduced kinetic energy of the emitted photoelectrons (~3.35 eV) is consistent with the averaged observed open circuit voltage $\langle V_{oc}\rangle$=−3.0±0.2 V. The positive photocurrent values for V_s=0 (i.e., similar to a short-circuit current I_{sc}) suggest that the photoelectrons are mainly emitted from the tungsten tip rather than the Si surface [B arrow in Fig. 3(c)]. Indeed, in our experimental conditions, positive current values indicate that the observed photoinduced electron signal is mainly originating from the STM tip. This can be explained by the very high reflectivity of the silicon surface (R~90%) at 157 nm.[31] Finally, the linear variation of the I_{sc} values as a function of the laser intensity [see the right inset in Fig. 3(c)] further indicates that the transient signal observed in Fig. 3(a) is due to a pure photoelectron emission strongly decoupled from photoinduced thermal heating.[12]

The absence of thermally induced STM-tip expansion cannot be explained by a classical two-temperature model.[32]

Indeed, when using this type of model with our experimental conditions, we can expect an STM-tip expansion of several nanometers per VUV laser pulse, which noticeably does not correspond to our measurements. Here, we emphasize that, although not observable, the VUV photoinduced STM-tip expansion can be very weak. Considering our detection limit on the feedback signal, this expansion can be estimated to be less than 15 pm per laser pulse. Furthermore, this very low photoinduced thermal expansion cannot be barely ascribed to the slight difference of the tungsten reflectivity, for *p* polarization, between 157 nm ($R \sim 0.2$) and 740 nm ($R \sim 0.3$). Although the absence of observable VUV photoinduced STM-tip expansion is not completely understood, our result suggests that the measured linear (i.e., one photon) photoelectronic emission might be related to a low electron-phonon coupling at the tungsten surface of the STM tip.[33] Indeed, these direct interband transition photoelectrons are usually considered as surface photoelectrons (the skin depth for tungsten at 157 nm is $\delta \sim 10$ nm). Thus, depending on the tungsten crystal orientation at the STM-tip surface, these photoelectrons are usually considered as unscattered, leading to potentially weak inelastic transitions to phonons.[33,34] Obviously, a complete description of these phenomena will need a detailed theoretical analysis, which is beyond the scope of this paper.

IV. CONCLUSION

In summary, our work shows that combining pure VUV wavelength light to an STM junction reduces considerably the photoinduced thermal STM-tip expansion compared to visible or IR wavelengths. By triggering the laser shots with the STM-tip scan motion, the time scale of the photothermal effects can be decoupled from the photoelectronic processes. Following optical separation from spurious emission, we observed that the optical excitation of the STM junction with pure VUV radiation induces rapid transient signals in the tunnel current that does not depend on the tip-surface distance while varying linearly with the incident laser intensity. Simulation of the transient response of our current measurement chain combined with the linear dependency of the photoelectron emission as a function of the laser intensity is a strong indication of low VUV induced electron-phonon coupling processes. This combination of lithographic short wavelength with a local probe microscope shows that the expected confined VUV optical field at the STM-tip apex can be used in a near-field regime, decoupled from thermal and electronic photoinduced processes. Such experiments will lead the way to investigating very high resolution optically induced surface interaction at the nanoscale.[35]

ACKNOWLEDGMENTS

D.R. would like to thank M. C. Castex and S. Chenais from Laboratoire de Physique des Lasers, Université Paris Nord, France, for the loan of a very high quality MgF_2 Pellin-Brocca prism.

*Corresponding author; damien.riedel@u-psud.fr

[1] S. Grafström, J. Appl. Phys. **91**, 1717 (2002).
[2] M. Völcker, W. Krieger, and H. Walther, Phys. Rev. Lett. **66**, 1717 (1991).
[3] H. Shigekawa, S. Yoshida, O. Takeuchi, M. Aoyama, Y. Terada, H. Kondo, and H. Oigawa, Thin Solid Films **516**, 2348 (2008).
[4] C. H. Schwalb, M. Lawrenz, M. Dürr, and U. Höfer, Phys. Rev. B **75**, 085439 (2007).
[5] V. Gerstner, A. Knoll, W. Pfeiffer, A. Thon, and G. Gerber, J. Appl. Phys. **88**, 4851 (2000).
[6] S. W. Wu, N. Ogawa, and W. Ho, Science **312**, 1362 (2006).
[7] A. Cvitkovic, N. Ocelic, J. Aizpurua, R. Guckenberger, and R. Hillenbrand, Phys. Rev. Lett. **97**, 060801 (2006).
[8] R. Huber, M. Koch, and J. Feldmann, Appl. Phys. Lett. **73**, 2521 (1998).
[9] S. Grafström, P. Schuller, J. Kowalski, and R. Neumann, J. Appl. Phys. **83**, 3453 (1998).
[10] L. Kronik, L. Burstein, Y. Shapira, and M. Oron, Appl. Phys. Lett. **63**, 60 (1993).
[11] C. C. Williams and H. K. Wickramasinghe, Nature (London) **344**, 317 (1990).
[12] I. Lyubinetsky, Z. Dohnálek, V. A. Ukraintsev, and J. T. Yates, J. Appl. Phys. **82**, 4115 (1997).
[13] M. Merschdorf, W. Pfeiffer, A. Thon, and G. Gerber, Appl. Phys. Lett. **81**, 286 (2002).
[14] A. V. Bragas, S. M. Landi, and O. E. Martínez, Appl. Phys. Lett. **72**, 2075 (1998).
[15] Z. B. Wang, B. S. Luk'yanchuk, L. Li, P. L. Crouse, Z. Liu, G. Dearden, and K. G. Watkins, Appl. Phys. A: Mater. Sci. Process. **89**, 363 (2007).
[16] O. J. F. Martin and Ch. Girard, Appl. Phys. Lett. **70**, 705 (1997).
[17] F. H'dhili, R. Bachelot, G. Lerondel, D. Barchiesi, and P. Royer, Appl. Phys. Lett. **79**, 4019 (2001).
[18] A. Chimmalgi, C. P. Grigoropoulos, and K. Komvopoulos, J. Appl. Phys. **97**, 104319 (2005).
[19] K. Dickmann, J. Jersch, and F. Demming, Surf. Interface Anal. **25**, 500 (1997).
[20] L. Cui, S. Mahajan, R. M. Cole, B. Soares, P. N. Bartlett, J. J. Baumberg, I. P. Hayward, B. Ren, A. E. Russell, and Z. Q. Tian, Phys. Chem. Chem. Phys. **11**, 1023 (2009).
[21] A. Saito, J. Maruyama, K. Manabe, K. Kitamoto, K. Takahashi, K. Takami, S. Hirotsune, Y. Takagi, Y. Tanaka, D. Miwa, M. Yabashi, M. Ishii, M. Akai-Kasaya, S. Shin, T. Ishikawa, Y. Kuwahara, and M. Aono, Jpn. J. Appl. Phys., Part 1 **45**, 1913 (2006).
[22] D. Riedel, A. J. Mayne, and G. Dujardin, J. Phys. IV **127**, 151 (2005).
[23] D. Riedel, A. J. Mayne, and G. Dujardin, Phys. Rev. B **72**, 233304 (2005).
[24] A. J. Mayne, D. Riedel, G. Comtet, and G. Dujardin, Prog. Surf. Sci. **81**, 1 (2006).
[25] M. Mehlhorn, H. Gawronski, L. Nedelmann, A. Grujic, and K.

Morgenstern, Rev. Sci. Instrum. **78**, 033905 (2007).
[26] K. Stokbro, C. Thirstrup, M. Sakurai, U. Quaade, B. Y. K. Hu, F. Perez-Murano, and F. Grey, Phys. Rev. Lett. **80**, 2618 (1998).
[27] E. T. Foley, A. F. Kam, and J. W. Lyding, Phys. Rev. Lett. **80**, 1336 (1998).
[28] S. I. Anisimov, B. L. Kapeliovich, and T. L. Perel'man, Sov. Phys. JETP **39**, 375 (1974).
[29] H. Wern and R. Courths, Surf. Sci. **162**, 29 (1985).
[30] M. W. J. Prins, M. C. M. M. van der Wielen, R. Jansen, D. L. Abraham, and H. van Kempen, Appl. Phys. Lett. **64**, 1207 (1994).
[31] *Vacuum Ultraviolet Spectroscopy*, edited by J. A. Samson and D. L. Ederer (Academic Press, San Diego, CA, 2001).
[32] P. J. Geshev, S. Klein, and K. Dickmann, Appl. Phys. B: Lasers Opt. **76**, 313 (2003).
[33] B. Feuerbacher and N. E. Christensen, Phys. Rev. B **10**, 2373 (1974).
[34] Z. Lin, L. V. Zhigilei, and V. Celli, Phys. Rev. B **77**, 075133 (2008).
[35] C. Girard, O. J. F. Martin, and A. Dereux, Phys. Rev. Lett. **75**, 3098 (1995).